Dynamics of Model Networks: The Role of the Melt Entanglement Length

Edgardo R. Duering

Max Planck Institut für Polymerforschung, 55021 Mainz, Germany, and Institut für Physik, Universität Mainz, 6500 Mainz, Germany

Kurt Kremer*

Institut für Festkörperforschung, Forschungszentrum Jülich, 52425 Jülich, Germany

Gary S. Grest

Corporate Research Science Laboratory, Exxon Research and Engineering Company, Annandale, New Jersey 08801

Received September 28, 1992
Revised Manuscript Received April 9, 1993

Polymer networks have been the subject of intense research for many years.[1-4] In spite of a very significant effort, many questions still remain unsolved. The main reason for this can be found in the difficulty in relating experimental data to structural properties and to analytical theory in a unique way. Theory has only been able to take structural properties into account in a rather crude manner. Experimentally the strands between cross-links in a network usually are highly polydisperse. While this can be incorporated within the random resistor network analogy,[5] the topology of the network has not been directly or explicitly incorporated into any theory. The most ambitious attempt to do so is due to Edwards et al.[3,6] His tube model and its variants, which led to the development of the reptation model for polymer melts, are the only approaches which attempt to incorporate the topology explicitly. The main idea in Edwards's approach is that on intermediate time scales a polymer melt and a polymer network should behave in a very similar way. Thus the entanglement length N_e, as defined for polymer melts, should also play a key role for networks whenever the strand length $N_s > N_e$. A direct test of this hypothesis, however, is experimentally not yet possible while our present simulations clearly demonstrate this.

Recently, two of the present authors[7] studied the reptation problem using extensive molecular dynamics simulation for chain lengths up to 200 monomers. For the model and system parameters employed, $N_e \approx 35$ monomers. Entanglement effects were found to be important for $N > N_c \approx 2N_e$ with strong effects of the free ends. Thus we have an efficient simulation model for which the dynamic properties of the melt are well-known and which can be used to study the properties of polymer networks. This was done for randomly cross-linked polymer melts in ref 8. In that study we used three different interaction potentials to test various theoretical models. These included a simple random-walk network, an excluded-volume interaction in which chains could not pass through each other, and a modified excluded-volume interaction, in which the effective excluded-volume interaction was conserved but the chains could pass through each other. There we found that, even for an average strand length $\langle N_s \rangle$ with $N_e/N_s \approx 3$, the conservation of the topology was extremely important and changed the elastic modulus by approximately 30%.[8] However, the large polydispersity of N_s makes it difficult to directly test the Edwards picture. Due to computer time limitations, we were not able to extend the results to the limit $\langle N_s \rangle > N_e$. This complication probably came from the effect of dangling chain ends and even a few small dangling clusters, which are expected not to support stress but in fact effect the relaxation behavior significantly. For them an exponentially slow relaxation is predicted.[9] To more directly compare our simulation results to theoretical models and experiment, we have carried out additional studies for end-cross-linked polymer melts in which the strand length is monodisperse. In an earlier study,[10] we examined the kinetics of the end-crosslinking process. Here we present new results for the dynamics of these systems, after the cross-linking was completed.

Starting from an equilibrated linear polymer melt of $MN = 30\,000$–$50\,000$ monomers at a density $\rho = 0.85\sigma^{-3}$, $^1/_4$ of the chain ends were identified randomly as tetrafunctional cross-linkers. N is the number of monomers per chain, while M gives the total number of chains. The system was then allowed to evolve with an excluded-volume interaction in the form of a repulsive Lennard-Jones potential between all monomers.[7] Whenever a free end came within a short reaction radius of $r_x = 1.3\sigma$ of an unsaturated cross-linker, the chain ends were attached. For the stoichiometric case considered here, the time dependence of the number of free ends decays as a power law, t^{-a}, with $a \approx 0.5$.[10] For the present study, we took one configuration for each chain length $N = 12$, 25, and 50 with $MN = 30\,000$ and one system of $N = 100$ with $MN = 50\,000$. A second $N = 100$ sample was tested to check the results. Within the error bars no deviations were observed. The simulation ran until at most about 2% of the ends remained free. We then stopped the cross-linking process and followed the dynamics of the cross-linked network. For the four systems studied, we covered the range from $^1/_3 \leq N_s/N_e \leq 2.9$. While the effect of the conserved topology for a randomly cross-linked system probably cannot directly be attributed to "entanglements" as defined dynamically in the reptation concept, we expect to observe the crossover toward this effect in the present samples. Note that polydispersity is negligible for the present case as each strand contains N bonds. Since the microscopic properties of our samples are well-known with practically no polydispersity of the strands, we do not suffer from the characteristic interpretation problems of the modulus.[4] The networks were studied using molecular dynamics simulations in which all the monomers are weakly coupled to a heat bath in order to keep the temperature stable.[7] Each system typically ran for $30\,000\tau$, where τ is the unit of time in standard Lennard-Jones units. For this model, the Rouse time of a chain of length N_e is approximately $\tau_R(N_e) \approx 1800\tau$.[7] Thus our simulation time exceeds the Rouse relaxation time of the longest primary chains ($N = 100$) significantly. Because there are almost no free ends, even the $N = 100$ chains are governed by the *in tube* relaxation, which is given by the Rouse time. In addition, we also rane the systems ($N \leq 50$) with no excluded-volume interaction, keeping only intrachain next-nearest-neighbor interactions along the chain. These simulated NRRW (nonreversal random walk) chains have a persistance length slightly smaller than the original chains. These reference systems can be compared to the phantom network model.

First consider the static properties of the primary chains after the cross-linking procedure was halted. For the original melts, the end-to-end distance of the chains scales as $\langle R^2(N) \rangle \approx 1.7\sigma^2 N$, where σ is the unit of length for the Lennard-Jones interaction and $c_\infty = 1.7$ is the Flory stiffness parameter.[7] We found that $\langle R^2(N) \rangle$ and the mean-square radius of gyration, $\langle R_G^2(N) \rangle$, were only marginally larger than for the equilibrated melt[7] (see Table I). The very small deviations indicate that only a very few chains, if at all, were significantly stretched due to the

0024-9297/93/2226-3241$04.00/0

Table I. Properties of the Model Networks for the NRRW (Nonreversal Random Walk) and the SAW (Self-Avoiding Walk) Networks[a]

	500/100	600/50		1200/25		2500/12	
M/N	SAW	SAW	RW	SAW	RW	SAW	RW
G°	0.019 ± 0.001	0.0257 ± 0.001	0.0094 ± 0.0001	0.034 ± 0.001	0.0190 ± 0.0001	0.070 ● 0.001	0.0396 ± 0.0001
G°_{TH}	0.0075	0.0157	0.0074	0.0320	0.0156	0.0654	0.0306
$\langle N_s \rangle$	100.5	50.4		25.4		12.04	
p_{es}	0.938	0.932		0.956		0.926	
$\bar{f}$	3.87	3.89		3.95		3.95	
ν	462	555		1145		2308	
μ	243	293		596		1229	
N_2	7	4		2		8	
N_3	30	26		28		56	
N_4	213	267		568		1173	
M_{free}	2	1		1		2	
M_{end}	20	19		18		50	
g_2^m/σ^2	≈35	24 ± 1	54.6 ± 1	18.0 ± 0.5	26.4 ± 0.5	10.8 ± 0.2	13.4 ± 0.1
g_2^x/σ^2	≈17	13.1 ± 0.5	42.1 ± 0.5	10.7 ± 0.3	20.6 ± 0.2	7.3 ± 0.2	11.0 ± 0.1
$\langle R^2 \rangle/\sigma^2$	174.4	90.4	63.9	44.5	33.4	19.1	14.7
$\langle R_G^2 \rangle/\sigma^2$	29.5	14.8	9.4	6.9	4.9	2.98	2.28

[a] The original melts consisted of M chains of N monomers, which we designate as M/N. The gel fraction is almost 100% as indicated by the number of free chains M_{free}. The number of free ends in the gel is M_{end}. The monomer density $\rho = 0.85\sigma^{-3}$. The mean active strand length $\langle N_s \rangle$ is slightly larger than N, because there are a few two-functional cross-links within the active cluster which have an active strand of length $2N_s$. The theoretical modulus G°_{TH} is determined from eq 1 with $h = 1$ for the phantom case which can be compared to the RW and $h = 0$ for the affine model for SAW networks. p_{es} is the fraction of elastically active monomers. $\bar{f}$ is the average functionality of the active cross-links ($f \geq 3$), and N_i, $i = 2$ and 4, are the number of cross-links with i ends attached in the elastically active backbone. g_2^m is the asymptotic value for the mean-square displacements of middle monomers of the chains in the active cluster and g_2^x is the corresponding result for the cross-links.

cross-linking process. The random walks, however, contract significantly causing strong density fluctuations, which are not possible when the excluded-volume interactions are present. In both cases $\langle R^2 \rangle \propto N$ is reasonably well satisfied.

For the present short paper we mainly confine our analysis to the modulus $G(t)$. To calculate $G(t)$, we measure the autocorrelation function $\langle \tilde{X}_p(t)\, \tilde{X}_p(0) \rangle / \langle X_p^2 \rangle$ of the Rouse modes $\tilde{X}_p$ of chains of length $N = 100$ ($N = 200$ for $N_s = 100$).[8,11] This is done by sampling the autocorrelation functions for many paths through the network, which have the mentioned length. It allows a rather simple estimate of the modulus without actually deforming the network. The time-dependent modulus $G(t)$ is given by[12]

$$G(t) = \frac{\rho k_B T}{N} \sum_{p=1}^{\infty} \frac{\langle \tilde{X}_p(2t)\, \tilde{X}_p(0) \rangle}{\langle X_p^2 \rangle} \qquad (1)$$

where N is the length of the constructed chain. The plateau modulus is defined by $G^\circ = \lim_{t\to\infty} G(t)$, which in the standard affine model or reptation picture should be equal to $\rho k_B T/N_s$ for $N_s < N_e$, N_s being the strand length between elastically active cross-links. To estimate the modulus by such an approach, we have to assure that the constructed chains are random walks so that the Rouse modes are eigenmodes of these constructed chains. One also needs to take care not to use closed loops. For the 500/100 sample we actually took the original chains and constructed walks of length $N = 200$. The results of both calculations coincide. In the present case the above criteria are fulfilled and we found that $\langle X_p^2(0) \rangle \propto N/p^2$ and $\langle X_{p=1}^2 \rangle \approx \langle R^2(N) \rangle / 2\pi^2$, where $\langle R^2(N) \rangle$ is the mean-square end-to-end distance of unperturbed melt chains. Thus the modulus, as for the entangled melt case, is given by eq 1, up to constant prefactors of order $O(1)$.

The inset in Figure 1 shows the result for $G(t)$ for the four systems with excluded-volume interaction potentials. The data clearly exhibit a decay to a plateau value, which can easily be determined. Note that a log–log plot is extremely sensitive to detect a residual decay. The results are included in Table I. This is to be compared to the various model predictions for the modulus. The two

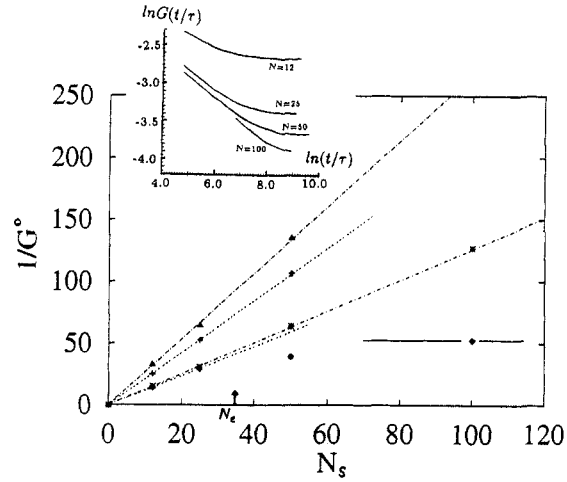

Figure 1. Inverse plateau modulus $1/G^\circ$ vs chain length N_s for all samples. The upper broken line gives the phantom network prediction (eq 1 (triangles), $h = 1$ ($T_eG^\circ_N = 0$)). The next line gives a fit of the measured moduli of the NRRW system (crosses). The third line shows the predictions of the affine model ($h = 0$) (with $T_eG^\circ_N = 0$) from the density of active strands (stars). The lowest line shows a fit to the two shorter SAW chains for the measured moduli of the SAW systems (diamonds). The melt entanglement length $N_e = 35$ is indicated. All models give $1/G^\circ = 0$ as $N_s \to 0$ except for the SAW case with $N = 50$ and 100. The straight line indicates the plateau region as suggested by the $N = 100$ result. The inset shows a ln–ln plot of the time-dependent modulus $G(t)$ as defined by eq 1 vs time for the four samples with excluded-volume interaction, as indicated.

standard models, the phantom network model and the affine deformation model, can be written as

$$G^\circ = \frac{k_B T}{V}(\nu - \mu h) + T_e G^\circ_N \qquad (2)$$

with k_BT Boltzmann's constant times temperature, ν the number of elastically active strands, μ the number of elastically active cross-links, and h a numerical constant between zero and 1.[13] $h = 1$ corresponds to the phantom network model and $h = 0$ to the affine model. The average functionality of the active cross-links is included in Table I. $T_eG^\circ_N$ is the trapping contribution due to the non-crossability of the chains. G°_N is the plateau modulus for

the un-cross-linked melt, and T_e is the trapping factor. Since we have a simple end-cross-linked network, there are no ambiguities in the definition of μ and ν as for the randomly cross-linked networks.[8] μ is just the number of cross-links with at least three paths to the infinite network, while ν is the number of strands between active cross-links. μ and ν as well as the fraction p_{ea} of monomers which are elastically active are given in Table I. It should be noted that ν and μ are analyzed for each given network, leaving no possibility of adjustments or fitting! Since one would only expect to find an effect of trapping for $N_s > N_e$, we expect to observe some indication for the present cases. In our previous study on randomly cross-linked melts,[8] we found in fact that the contribution from the conserved topology was nonzero even for networks constructed from melts with $N = 50$ and $\langle N_s \rangle \approx N_e/3$. An interesting question is to what extent do the present networks follow the classical models. If we disregard the trapping contribution, we can calculate the plateau moduli for the classical models from eq 2 using the actual values of ν and μ. First consider the random-walk data. One would expect for this case that the data should be described by the phantom network model. The simulation, however, gives a value which is slightly too large. What is consistent, however, is that in both cases the result of the phantom model and G° determined from the relaxation data are strictly proportional to the inverse strand length N_s. The reason for this deviation probably is 2-fold. First, the chains are not perfect random walks. Second, the system can be viewed as a small disordered harmonic solid, in which there may be significant finite size effects, which can reduce the fluctuations. Both effects eventually might increase the modulus.

Now consider the more interesting case with excluded-volume interactions which conserve the topology. Here the finite size effects are expected to be much weaker because of the much stronger coupling of the particles. We already know of the general importance of conserved topology from our previous study.[8] However, there the physical mechanism is not entirely clear. Table I contains our results for the end-cross-linked system. G°_{TH} is the theoretical result for the affine network model ($h = 0$) which agrees well with G° obtained from $G(t)$ for $N = 12$ and 25. The deviation, although systematic, is a little less than 10% and points toward the same direction as for the randomly cross-linked melts. More importantly we find the expected ratio, $G^\circ(N_s = 12)/G^\circ(N_s = 25) \approx 25/12$. Effects of the topology do not show up as a difference in the N-dependency of G° for these two systems. The effects of the conserved topology are becoming dominant however for $N_s = 50$, 100. The plateau modulus is significantly larger by 63% than expected from the affine model without trapping for $N_s = 50$. For $N_s = 100$ we find an increase of about 155%. Thus we observe a dramatic effect of the strand length. Comparing this result with the short chains and the random-walk case, we conclude that this difference has to be due to the fact that $N_s > N_e$. A detailed discussion of the trapping contribution will be published elsewhere.[14] To illustrate this more clearly, we combine all our data in Figure 1. One clearly sees that $1/G^\circ \propto N_s$ for the NRRW case and the SAW case for $N_s < N_e$, while for $N_s > N_e$ the SAW data deviate significantly. Lines are included to better visualize the results. The apparent bending over for the chains with excluded-volume interaction from an affine-like behavior toward a plateau obviously starts around the melt entanglement length $N_e = 35$. From this result, we expect a modulus which is almost independent of N_s for even larger strand lengths. This will be studied systematically for this and even more idealized networks in a future publication.[14]

The general picture developed here is supported by the mean-square displacements $g_2(t)$ for the middle monomers of the chains and for the cross-links. As expected for both the middle monomers and the cross-links, the maximum displacement for long times, $g_2 \propto N_s$ for the random walks, while this is not the case for the SAW's. There we find a very pronounced confinement of the monomer displacement. For $N_s = 50$, $g_2^m = 24\sigma^2$ and $g_2^m = 35\sigma^2$ for $N_s = 100$ for the inner monomers. From the reptation analogy one would expect[7,11,12] a value of $2R_G^2(N_e)(N_s/N_e)^{1/2} \approx 22\sigma^2(N_s/N_e)^{1/2}$ which again very well fits our present results. This can be compared to the neutron spin-echo data of Oeser et al.[5] However, using τ_e to calibrate the times,[7] their data cover significantly shorter times than the present simulations. Their data do not significantly deviate from Rouse relaxation with a somewhat enhanced friction.

To conclude, we presented data from a molecular dynamics simulation, which directly show the importance of chain entanglements, as they are defined by the dynamics of the un-cross-linked melts. The data strongly support the view that for $N_s \gg N_e$ the plateau modulus should be independent of N_s. This shows that the trapped entanglements can contribute to the modulus well beyond simply suppressing the junction fluctuations. Together with our previous investigation of randomly cross-linked polymer melts we find that the conserved topology gives rise to two different effects. First the modulus is enhanced by an N_s independent factor due to the conservation of topology even for very short chains. The available configurations are significantly reduced compared to simple packing requirements. This effect seems to be independent of chain length, as to be expected from a local constraint. The second effect is due to the same constraint as the dynamic entanglement effect in melts, where the physical consequences are explained by the reptation picture. To our knowledge, it is the first time these effects have clearly been demonstrated by simulation or experiment. Our results are in agreement with recent experiments[16] on model networks which qualitatively suggest the importance of trapped entanglements even for N_s in the range of N_e.

Acknowledgment. This research was supported by a generous grant of cpu time from the German supercomputer center HLRZ, Jülich, Germany. E.R.D. acknowledges support from SFB262 of the Deutsche Forschungsgemeinschaft DFG. K.K. and G.S.G. acknowledge support through a NATO travel grant and discussions with R. Eueraers, W. W. Graessley, and G. ver Strate.

References and Notes

(1) Treolar, L. R. G. *Theory of Rubber Elasticity*; Oxford University Press: Oxford, U.K., 1949.
(2) Flory, P. J. *Proc. R. Soc. London, Ser. A* **1976**, *351*, 351.
(3) Edwards, S. F.; Vilgis, T. A. *Rep. Progr. Phys.* **1988**, *51*, 243 and references therein.
(4) Mark, J. E. *Adv. Polym. Sci.* **1982**, *44*, 1.
(5) Higgs, P. G.; Ball, R. C. *J. Phys. (Paris)* **1988**, *49*, 1785.
(6) Edwards, S. F. *Proc. Phys. Soc.* **1967**, *92*, 9.
(7) Kremer, K.; Grest, G. S. *J. Chem. Phys.* **1990**, *92*, 5057; **1991**, *94*, 4103(E). Kremer, K.; Grest, G. S.; Carmesin, I. *Phys. Rev. Lett.* **1988**, *61*, 586.
(8) Duering, E. R.; Kremer, K.; Grest, G. S. *Phys. Rev. Lett.* **1991**, *67*, 3531; and to be published.
(9) Curro, J. G.; Pincus, P. A. *Macromolecules* **1983**, *16*, 559.
(10) Grest, G. S.; Kremer, K.; Duering, E. R. *Europhys. Lett.* **1992**, *19*, 195.

(11) Kremer, K.; Grest, G. S. *J. Chem. Soc., Faraday Trans.* **1992**, *88*, 1707.
(12) Doi, M.; Edwards, S. F. *The Theory of Polymer Dynamics*; Oxford University Press: Oxford, U.K., 1986.
(13) Pearson, D. S.; Graessley, W. W. *Macromolecules* **1978**, *11*, 528. Langley, N. R. *Macromolecules* **1968**, *1*, 348.
(14) Everaers, R.; Kremer, K., in preparation. Everaers, R.; Grest, G. S.; Kremer, K.; Duering, E. R., in preparation.
(15) Oeser, R.; Ewen, B.; Richter, D.; Farago, B. *Phys. Rev. Lett.* **1991**, *67*, 3534.
(16) Patel, S. K.; Malone, S.; Cohen, C.; Gillmor, J. R.; Colby, R. H. *Macromolecules* **1992**, *24*, 5241.